Appl. Phys. B 63, 349–354 (1996)

Applied Physics B Lasers and Optics

Laser action of $nd^8(n+1)s^2 - nd^9(n+1)p$ transitions in HgIII, CuII and AgII

K.B. Blagoev, G. Popov, E. Dimova

Institute of Solid State Physics, Tzarigradsko Chaussee 72, 1784 Sofia, BULGARIA,
(Fax: +359 – 2/9753236, E-mail: kblagoev@bgearn.acad.bg

Received: 23 August 1995/accepted: 12 April 1996

Abstract A mechanism of the laser action of $5d^8\,6s^2$ –$5d^9\,6p$ HgIII transitions is proposed. The explanation is based on atomic constants of the transitions and the predominant role of direct electron excitation of the upper laser level. The kinetic models of electron beam and hollow cathode discharge sources are calculated. The theoretical estimations are compared with experimental data and possible laser transitions are also proposed. The role of electron impact excitation in the formation of inverse population for two-electron transitions in CuII and AgII obtained in hollow cathode discharges is discussed.

PACS: 42.55 Hq, 52.20.-j, 34.80.-i

There are several papers in the literature where $nd^8(n+1)s^2 - nd^9(n+1)p$ laser transitions were observed in the spectra of HgIII, CuII, AgII [1–5]. In these experiments, the noble gases He, Ne were used as admixture. Different types of gas discharges were used – pulse positive column discharge (HgIII) and hollow cathode discharge (CuII, AgII).

The possible mechanism of population inversion between $nd^8(n+1)s^2$–$nd^9(n+1)p$ states was discussed in [6], based on the data about radiative lifetimes of $nd^8(n+1)s^2$ states and the excitation of these states by electron impact as well as the transition probabilities of $nd^8(n+1)s^2$–$nd^9(n+1)p$ transitions. Up to now, there is no definite explanation of the inverse population mechanism of these transitions.

Here, as a basic mechanism we propose an electron impact excitation of the upper laser level from the ground state. This mechanism could play the main or additional role in different cases. Our consideration relies on the data of atomic constants of the upper and lower laser levels. We also discuss the possibility to observe laser action at various experimental conditions in different types of discharges.

1 Discussion

There are two papers in which the laser action of HgIII states was observed. In the first paper [1], a pulse HV discharge in Hg + He mixture was used. The 4797 Å ($5d^8\,6s^2\,1\,2_4$–$5d^9\,6p\,2\,3^0_3$) spectral line of HgIII was observed along with 6150 Å, 5677 Å transitions of HgII. The HgIII laser action maximum of 4797 Å was observed when He gas pressure was decreased to zero. In the second paper [2], a spectral line in HgIII at 6501 Å ($5d^8\,6s^2\,1\,1_1$–$5d^9\,6p\,1\,2^0_1$) was observed. The experiment was carried out in pure mercury vapor. The tables given in [7] and the papers cited there were used for the designation of excited states and spectral line classifications.

The structure of the HgIII spectrum and the atomic constants of the HgIII excited levels allow to propose an explanation for the formation of population inversion.

The $5d^8\,6s^2$ electron configuration is formed when two electrons from the inner $5d^{10}$ shell are removed. Strong spectral lines, which connect the $5d^9\,6s$ and $5d^8\,6s^2$ configurations, were observed even though these transitions are two electron ones [8]. This experiment was carried out in a hollow cathode cw discharge.

The radiative lifetimes of $5d^8\,6s^2$ were measured [9] using the delayed coincidence method and pulse electron excitation. The experiment was carried out in a diffusion cell at mercury pressure in the range from 10^{-5} to 10^{-1} Torr and electron beam intensity up to 1.7 A/cm^2. The results are presented in Table 1. The experimental results are confirmed by theoretical calculation [10] which is performed by multiconfigurational Hartree-Fock approximation, taking into account electron configuration mixing. Practically, due to this mixing both the $5d^8\,6s^2$–$5d^9\,6p$ and the $5d^9\,6p$–$5d^9\,6s^2$ transitions are possible. By measuring the intensities of all $5d^8\,6s^2$–$5d^9\,6s$ spectral lines, the corresponding transition probabilities were obtained [9]. The $5d^8\,6s^2$–$5d^9\,6p$ transition probabilities are also presented in Table 1. At high electron excitation energies (150–300 eV), the intensities of corresponding spectral lines have large values, comparable with those of strong atomic lines. This fact is due to the large cross-section of electron impact excitation of $5d^8\,6s^2$ states from

Table 1. Radiative lifetimes [ns], transition probabilities (A_{ik}) [10^5 s^{-1}], effective cross-sections (Q_{ik}) [10^{-18} cm^2] and excited-state cross-sections (Q_i) [10^{-18} cm^2] of HgIII $5d^8\,6s^2$ states

State	E [cm^{-1}]	Transition	λ [Å]	τ_i	A_{ik}	Q_{ik}	Q_i
11_2	118926	1_2–1_2^0	6501	2480	3.55	0.14	0.16
	122735	1_2–2_3^0	7517		0.48	0.02	
10_1	126468	10_1–1_2^0	5210	1660	6.00	0.18	0.18
12_4	133731	2_4–2_3^0	4797	2100	4.76	1.30	1.30
13_2		3_2–1_2^0	3312	2250	2.43	0.19	0.35
		3_2–2_3^0	3557		1.62	0.12	
		3_2–3_2^0	6584		0.26	0.03	
		3_2–4_1^0	6610		0.13	0.01	
		3_2–6_2^0	7808		0.20	0.02	
14_0	158909	4_0–8_1^0	3090	473	20.6	0.14	0.14

Table 2. Radiative lifetimes of HgIII of $5d^9\,6p$ states [ns]

State	E [cm^{-1}]	Transition	λ [Å]	τ (experiment)	τ (theory)
$^3D_1$	134998	$5d^9\,6p\,^3D_1$–$5d^{10}\,^1S_0$	740.75	0.90	0.70; 0.63
$^1P_1$	126556	$5d^9\,6p\,^1P_1$–$5d^{10}\,^1S_0$	790.17	0.52	0.28; 0.26
$^3P_1$	118607	$5d^9\,6p\,^3P_1$ – $5d^{10}\,^1S_0$	843.11	1.20	1.00; 0.88

the ground atomic state [11], even though the electron shells are changed from $5d^{10}\,6s$ to $5d^8\,6s^2$. The electron excitation cross-sections of $5d^8\,6s^2$ states were also obtained [11] and are presented in Table 1.

Hence, the $5d^8\,6s^2$ states have, both, a large value of radiative lifetimes and a large value of cross-sections for electron impact excitation from the ground atomic state.

Recently, radiative lifetimes of the $5d^9\,6p$ state were measured using the beam-foil method. The transition probabilities of $5d^9\,6p$–$5d^9\,6s$ and $5d^9\,6p$–$5d^{10}$ transitions were also obtained [12]. These results are supported by theoretical calculations, performed by multiconfigurational Heartree-Fock approximation, taking into account electron configuration mixing [12]. These data are presented in Table 2.

It is necessary to point out some considerations, which arise from radiative lifetime and electron excitation experiments and which are important for the estimation of processes of population and depopulation of $5d^8\,6s^2$ and $5d^9\,6p$ states:

(i) In the $5d^8\,6s^2$ lifetime experiments [9], no cascade transitions from $5d^9\,6p$ states, which are the only possible ones [8], were observed. The $5d^9\,6p$–$5d^8\,6s^2$ and $5d^9\,6p$–$5d^9\,6s$ transitions were not observed [9] at experimental conditions – mercury vapor pressure up to 0.3 Torr and electron beam density up to 5 A/cm^2. Hence, at these experimental conditions the population of $5d^9\,6p$ states by direct electron excitation from ground mercury states is negligible.

(ii) In the papers devoted to spectral lines classification, where the hollow cathode discharge is employed, the spectral lines $5d^9\,6p$–$5d^8\,6s^2$; $5d^9\,6p$–$5d^9\,6s$ have intensities of the same order of magnitude as the $5d^8\,6s^2$–$5d^9\,6p$ transitions. Hence, one can suppose that in this case, at the experimental conditions of [8], the stepwise excitation of $5d^9\,6p$ HgIII states occurs.

Excitation functions and cross-sections of the $5d^8\,6s^2$ state for electron impact excitation from $5d^{10}\,6s$ Hg_0^+ and $5s^{10}$ Hg_0^{2+} states, which are also necessary to take into account in the discussion of population processes of HgIII states, were also measured [13].

Taking into account the structure of HgIII levels and atomic constants as well as the considerations which are mentioned above, we can propose the following processes of population and depopulation of $5d^8\,6s^2$, $5d^9\,6p$ excited HgIII states.

Let us suppose experimental conditions in which the mercury vapor pressure is less than 0.3 Torr. At these experimental conditions, the $5d^8\,6s^2$ states are populated by direct electron excitation from the ground $5d^{10}\,6s^2$ atomic mercury state. The cascade transitions from $5d^9\,6p$ could be neglected.

Depopulation of $5d^8\,6s^2$ states is due to the $5d^8\,6s^2$–$5d^9\,6p$ states.

Population of $5d^9\,6p$ states is due to the cascade transitions from $5d^8\,6s^2$ states.

Direct electron excitation from the ground atomic state as well as stepwise electron excitation at these experimental conditions should be neglected.

Depopulation of $5d^9\,6p$ states is due to the $5d^9 6p$ –$5d^9\,6s$, $5d^{10}$ radiative transitions, which have large probabilities (Table 2).

Hence, the same processes govern the population and depopulation of $5d^8\,6s^2$ and $5d^9\,6p$ states, but they have different probabilities for states of both electron configurations. Because of this fact the population inversion of the above-mentioned electon configurations is formed.

In order to obtain laser action, a sufficient concentration of excited HgIII $5d^8\,6s^2$ states should be achieved by devices in which there exist a large number of fast electrons – for example, e-beam, hollow cathode discharge, pulse positive column. For the above-mentioned methods,

additional processes such as atom–atom and electron–atom collision depopulation should be taken into account.

Further, a kinetic model for different type sources will be discussed and we will try to give an explanation of the laser action, which is obtained in Hg–Hg mixture [1] or pure mercury vapor media [2].

Kinetic model. A simple kinetic model of the Hg laser, operating on the HgIII 6501 Å line is proposed. A kinetic scheme for the processes is considered, which includes only two levels – an Upper Laser Level (ULL) and a Lower Laser Level (LLL). In the scheme, the following assumptions are made:

The ULL is populated through direct excitation by fast electrons from the ground state. It is depopulated through spontaneous emission, electron deexcitation and deexcitation via Hg atoms.

The LLL is populated by spontaneous emission and electron deexcitation of ULL, both coming from ULL, while depopulation of LLL is through spontaneous emission.

The balance equations for ULL, LLL, Hg and HgII, using e-beam excitation, are as follows:

$$dN_2/dt = \nu_{exc}[Hg] - (A_{eff} + \nu_{2,diff} + k_{deexc} n_e) N_2, \quad (1)$$

$$dN_1/dt = \nu_{2,sp} N_2 - (\nu_{2,sp} + \nu_{1,diff}) N_1, \quad (2)$$

$$d[Hg^+]/dt = \nu_{ion}[Hg] - \nu_{diff}[Hg^+], \quad (3)$$

$$[Hg_0] = [Hg] + [Hg^+], \quad (4)$$

where N_2 and N_1 are the ULL and LLL populations, respectively, n_e is the electron density, [Hg] is the ground-state Hg atom density, $[Hg^+]$ is the ground-state HgII density, k_{deexc} is the electron deexcitation rate constant, ν_{sp} are the spontaneous emission probabilities, ν_{ion} and ν_{exc} are the ionization frequency of Hg atoms by fast electrons and the excitation frequency of the ULL, respectively, ν_{diff}, $\nu_{1,diff}$ and $\nu_{2,diff}$ are the diffusion frequencies of HgII, LLL and ULL, respectively, and A_{eff} are the effective values of $5d^8 6s^2$–$5d^9 6p$ transition probabilities.

The Hg atom ionization and excitation frequencies by beam electrons are namely ν_{ion}, ν_{exc} [14]:

$$\nu_{ion} \cong 2(\bar{\sigma}_{ion}/e) * je, \quad (5)$$

$$\nu_{exc} \cong 2(\bar{\sigma}_{exc}/e) * je, \quad (6)$$

where $\bar{\sigma}_{ion} = [1/\varepsilon \int_0^{\varepsilon} d\varepsilon'/\sigma_{ion}(\varepsilon')]^{-1}$ and $\bar{\sigma}_{exc}$ are the averaged ionization and excitation cross-sections (σ_{ion} is taken from [16], σ_{exc} are measured in [11]), ε is the electron energy, e is the electron charge and j_e is the density of primary electrons.

The ionization and excitation by secondary electrons is accounted for by the introduction of factor 2. Taking into account that the electrons have energies of about 1 keV, a significant number (50–70%) of secondary and third generation electrons have energies higher than the ionization potential [17]. The stepwise ionization from Hg atom excited states also gives a small contribution. The factor 2 in (5) roughly describes the additional ionization due to these electrons.

In the HCD case, the total number of ionizations by fast electrons in the negative glow region $\nu_{ion}[Hg]V$ is equal to the particle current i/e, which is moving to the anode, where i is the current and V is the volume of active media [18]. Hence, the ionization frequency is

$$\nu_{ion} = i/e[Hg]V. \quad (7)$$

The ionization frequency can also be derived from the continuity equation $\nabla J_e/e = \nu_{ion}[Hg]$, where J_e is the particle current density. Multiplying both sides of this equation by factor $\pi R^2 L$, where R and L are the radius and length of the cathode, one can obtain $2\pi RLj/e = \nu_{ion}[Hg]\pi R^2 L$. Taking into account that $2\pi RLj/e = i/e$ and $V = \pi R^2 L$, one obtains (7).

The excitation frequency can be derived from (5), (6) and (7):

$$\nu_{exc} = (\bar{\sigma}_{exc}/\bar{\sigma}_{ion}))(i/e[Hg]V). \quad (8)$$

The electron deexcitation constant k_{deexc} could be estimated using [15]. The diffusion frequencies are calculated on the basis of the mobility of HgI in Hg [16].

Solving the balance equations, one can calculate the populations of ULL and LLL, the electron density as well as laser gain using the well-known formula $\chi = \sigma[N_2 - g_1/g_2 \cdot N_1]$, where σ is the phototransition cross-section and g_1, g_2 are the statistical weights of ULL and LLL.

2 Results

The calculations of laser gain for e-beam and HCD are performed. The dependence of the laser gain on Hg pressure for e-beam pumping at different current densities for the 6501 Å ($5d^8 6s^2\ 1_2$–$5d^9\ 6p2_3$) transition is shown in Fig. 1. With mercury pressure increase, the population of ULL also increases due to direct excitation by fast electron from the ground state. At high mercury pressure, the population of ULL decreases due to electron deexcitation. For low electron densities, depopulation of ULL through electron deexcitation is negligible, the A_{eff} value changes slowly and laser gain increases; the slow change of A_{eff} is also due to the $(Hg^{2+})^*$ + Hg deexcitation collisions. At very high current density, n_e reaches significant values

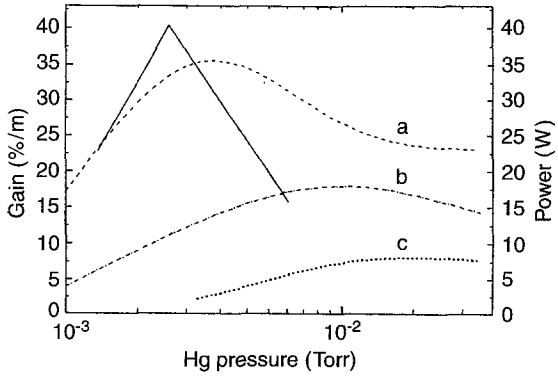

Fig. 1. The dependence of laser gain vs mercury vapour pressure calculated for 6501 Å ($5d^8 6s^2$–$5d^9 6p$) in the e-beam case (a – j = 300 A/cm^2; b – j = 100 A/cm^2; c – j = 30 A/cm^2). Solid line presents experimental results [2]

even at low Hg pressure (2–5 mTorr), the A_{eff} also increases rapidly. The optimal pressure is 2–10 mTorr, which is observed experimentally in [2], at $j \approx 400$ A/cm^2.

The dependence of the laser gain on mercury pressure in HCD is presented in Fig. 2. With mercury pressure decrease, the depopulation of ULL decreases and gain increases. But at very low pressures, an ambipolar diffusion of ULL takes place and ULL population rapidly decreases. If the mercury pressure is lower than a certain threshold value, the ambipolar diffusion of ULL becomes so considerable that the population of ULL is not sufficient for the creation of population inversion. The threshold and the optimal mercury pressure are 1 mTorr and 5–10mTorr, respectively.

The main difference between e-beam pumping and HCD is the dependence of ULL population on the mercury pressure. In the case of e-beam pumping, the total number of excitations of ULL per unit time and unit volume (7) is proportional to the mercury pressure, while in the case of HCD (8) it does not depend on the mercury pressure. That is why e-beam pumping is effective at intermediate and high pressures. It follows from expression (7) that at low pressure one should use higher current density [19].

It is worthwhile to mention that, although the current density in HCD is relatively small, the corresponding current is high enough. At 50 cm active media length and current density 3 A/cm^2, the current is 300 A. The comparison between longitudinal e-beam pumpint [2] and HCD shows that in both cases a current of 300 A is required.

The results of the kinetic model could be employed for explanation of laser action, obtained in [1, 2].

In [1], laser action on 4797 Å ($5d^8\,6s$–$5d^9\,6p$) was reported. The experiment was carried out in a quartz tube 1.2 m long and 6 mm in diameter. The 15 A current pulse, with 0.2 μs duration, was applied, in the Hg–He mixture Hg pressure was about 10^{-3} Torr, He pressure was 0.5 Torr. At least 2.5% gain was obtained. The laser pulses coincide with current pulses without any afterglow. The laser generation is observed, when the He pressure was sufficiently below initial 0.5 Torr. The conclusion was drawn that the He atoms could interfere with the 45 eV electrons, which are responsible for the laser action [1].

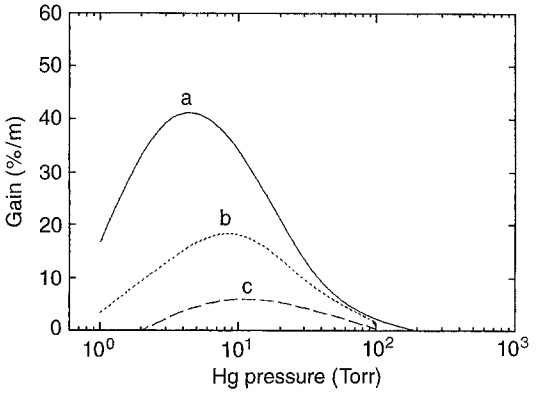

Fig. 2. The dependence of laser gain vs mercury vapour pressure calculated for 6501 Å ($5d^8\,6s^2$–$5d^9\,6p$) in the hollow cathode discharge case (a – $j = 30$ A/cm^2; b – $j = 3$ A/cm^2; c – $j = 1$ A/cm^2)

In [2], a 1.2 m tube with 10 mm diameter was used. The mercury vapor pressure was varied in the range 10^{-3}–2×10^{-2} Torr. The 300 A current pulses having 25 μs–2 ms duration were employed. The laser action of another spectral line 6501 Å ($5d^8\,6s^2\,1\,1_2$–$5d^9\,6p1_2^0$) HgIII was observed. The laser action pulses, but have smaller duration. For short 25 μs pulses, the optimum mercury pressure is about 2×10^{-3} Torr and no laser action for $p > 10^{-2}$ Torr was observed. The output power was 40 W. For long pulses (2 ms), the same values of output power were achieved, but the optimum mercury pressure was $p > 10^{-2}$ Torr.

From the experimental conditions cited in both papers, one could estimate the distance which electrons will cover before they stop:

$$L = \sum_e \lambda(e) \approx eU/E_{ei}\lambda(e), \tag{9}$$

where U is the applied voltage, E_{ei} is the energy of electron–ion couple creation, which for mercury is ≈ 25 eV, and $\lambda(\varepsilon)$ is the free path of electrons – $\lambda(\varepsilon) = 1/\sigma_{\text{tot}}(\varepsilon) \cdot N$ (at optimal mercury pressure 2×10^{-3} Torr, $U = 4.5$ kV [2] and $\sigma_{\text{tot}} = 2 \times 10^{-15}$ cm^2; $\lambda(\varepsilon) \approx 8$ cm; the total number of ionizations $z_{\text{tot}} = 180$; $L = z_{\text{ion}} \cdot \lambda(\varepsilon) \approx 1400$ cm) [13, 20]. Hence, in these experiments the electron beam conditions are fulfilled. From Fig. 1 in [2], where the output power dependence vs applied pulse voltage, at different mercury pressures, is pressented, one can extract the dependence of output power vs Hg atom pressure. This dependence has a sharp maximum at 2.5×10^{-3} Torr (Fig. 1). Hence, the experimental result is supported by theoretical calculations. The output power increases with the increase of mercury pressure. At mercury pressures greater than $\sim 3 \times 10^{-3}$ Torr, the deexcitation of $5d^8\,6s^2$ states by collisions with both mercury atoms and low-energy electrons takes place.

Further, the stepwise electron excitation of $5d^9\,6p$ low laser levels becomes substantial, which also destroys the population inversion.

The output power increases with pulse current and voltage increase (Fig. 1, [2]) since the population of the upper laser level is increasing. At higher pulse voltage or pulse current, the number of low-energy electrons is increased and the depopulation of the upper laser level by collisions with these electrons is increased. That is why the optimum of supplied voltage is at 4.5 kV. These collisions could be the reason for the sharp decrease of the output power pulses, while the maximum of laser and current pulses coincides (Fig. 2, [2]).

The gain coefficient for all $5d^8\,6s^2$–$5d^9\,6p$ transitions is also calculated in the e-beam case at current density 300 A/cm^2. Here we use A_{ik} transition probabilities instead of A_{eff}, which leads to the overestimation by not more than 20% of the calculated gain values. The wavelengths of these transitions are in the region 7808–3090 Å. The gain coefficients vs mercury vapor pressure are presented in Fig. 3. A group of transitions have gain coefficients approximately 10% or less. That is why from this group only the dependence of 3090 Å is presented. However, one can point out that transition

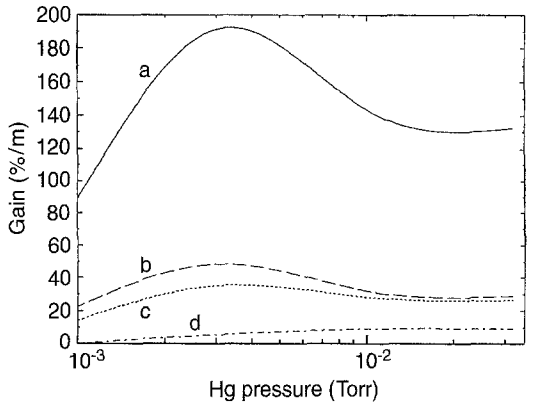

Fig. 3. The dependence of laser gain vs mercury vapour pressure calculated for the e-beam case at current density $j = 300$ A/cm^2 for $5d^8\,6s^2$–$5d^9\,6p$ transients (a – 4797 Å, b – 6501 Å, c – 5210 Å, d – 3090 Å)

5210 Å ($5d^8\,6s^2\,10_1$–$5d^9\,6p\,1_2^0$) has practically the same gain coefficient as 6501 Å. Hence, laser action could be expected on the 5210 Å transition at experimental conditions equal to those for the 6501 Å line.

Lasing on $5d^8\,6s^2$–$5d^9\,6p$ HgIII transitions could be realized using different type devices similar to e-beam, such as beam-type discharge with two parallel plate electrodes [23] as well as blumline-type transfer discharge.

The laser action on $nd^8(n+1)s^2 - nd^9(n+1)p$ intercombination transitions was also obtained in CuII and AgII spectra. In these cases the $nd^8(n+1)s^2$ states are also metastable. Their lifetimes are calculated from theoretical transition probabilities [10] and are presented in Table 3. Hollow cathode discharge and He–Cu mixture was used for this laser transition investigation [3]. The achieved laser transitions are:

$3d^8\,4s^2\,{}^3P_1$–$3d^9\,4p\,{}^3P_2^0$ – 4506 Å,

$3d^8\,4s^2\,{}^3P_2$–$3d^9\,4p\,{}^3P_2^0$ – 4555 Å,

$3d^8\,4s^2\,{}^3P_1$–$3d^9\,4p\,{}^3P_0^0$ – 5060 Å.

The Penning ionization was assumed in this case as a possible mechanism for the creation of population inversion. Here, we estimate the ratio between rates of direct electron excitation of $3d^8\,4s^2$ CuII states from ground state and Penning ionization.

$$\Gamma_{\text{exc}} = \nu_{\text{exc}} N_{\text{Cu}_0}, \tag{10}$$

$$\Gamma_{\text{pen}} = k_{\text{par.pen}} N_{\text{He}^m} N_{\text{Cu}_0}, \tag{11}$$

$$\eta = \Gamma_{\text{exc}}/\Gamma_{\text{pen}} = \nu_{\text{exc}}/k_{\text{par.pen}} N_{\text{He}^m}, \tag{12}$$

where ν_{exc} is the frequency of the electron excitation process, N_{Cu} is the number of Cu atoms, $k_{\text{par.pen}}$ is the partial rate constant for the excitation of $3d^8\,4s^2$ states by Penning ionization with He(2^3S) atoms.

There are no data for cross-section of the latter process in the literature. This constant could be estimated taking into account the cross-sections of K, Rb. On the other hand, it is well known that the partial constant of excitation of Beuthler states of ZnII, CdII consists of 0.1 from the total volume of Penning ionization cross-section. Using these estimations, we assume for $k_{\text{par.pen}} \approx 10^{-10}$ cm^3/s.

The He(2^3S) atom density is taken from [19] (Fig. 4, [19]), where the experimental conditions of hollow cathode discharge in Cu + He mixture are close to those of laser action experiments [3]. This value is estimated as $N_{\text{He}^m} = 9 \times 10^{11}$ cm^{-3}.

The cross-sections for electron impact excitation of $3d^8\,4s^2$ states are presented in Table 3 [21]. These values are the low limit, since some transitions were not measured.

The excitation frequency ν_{exc} is calculated taking into account the electrons which have energies greater than 31 eV (this is the threshold energy of $3d^8\,4s^2$ states). The estimated value is $\nu_{\text{exc}} \approx 8.8$ s^{-1}.

Taking into account all these values, the rate constant ratio is approximately $\eta \approx 1/8$. Hence, 10–20% of the population of the $3d^8\,4s^2$ state is due to the electron excitation mechanism and has to be taken into account.

The laser action on $4d^8\,5s^2$–$4d^9\,5p$ AgII transitions was obtained also in hollow cathode discharge in Ag + Ne mixture [4, 5].

The charge exchange process was assumed as the possible one for population inversion. There are no data for electron impact excitation of $4d^8\,5s^2$ AgII states, as well as for atom–atom collision cross-sections. That is why it is difficult to estimate the role of the discussed process of direct electron excitation of $4d^8\,5s^2$ states. However, in [22] the excitation of different AgII states in pulse Ag–He mixture was investigated and it was observed that the pulse of $4d^8 5s^2$–$4d^9\,5p$ spectral line intensities coincides with the current pulse. This fact could be related to the significant role of the direct electron excitation of $4d^8\,5s^2$ states.

3 Conclusion

The main reason for population inversion of $5d^8\,6s^2$–$5d^9\,6p$ HgIII transitions is the large probability of electron impact excitation of these states from the ground atomic state. This fact could be connected with experiments in which a laser action in the VUV region on

Table 3. Radiative lifetimes τ, transition probabilities A_{ik}, electron impact cross-sections Q_i of CuII states

State	Transition	λ (Å)	τ [s]	A_{ik} [s^{-1}]	Q_i [10^{-18} cm^2]
$4s^2\,{}^3P_1$	$4s^2\,{}^3P_1$–$4p\,{}^3P_0$	506.0	$> 10^{-5}$	$> 10^5$	0.134
	$4s^2\,{}^3P_1$–$4p^3P_2$	450.6			
$4s^2\,{}^3P_2$	$4s^2\,{}^3P_2$–$4p\,{}^3P_2$	455.6	$> 10^{-5}$	$> 10^5$	0.291
$4p^3D$			1.53×10^{-9}		3.64

$3d^8\,4s^2$–$3d^9\,4p$ ZnIII transitions was investigated [23, 24]. A population inversion was created by X-rays, which discard one of the $3p$ electrons. The following super Coster-Kronig transitions lead to some kind of selective population of the $3d^8\,4s^2\,{}^1G_1$ state. The amplification of several transitions close to 130 nm was observed.

Based on the data of different experiments, it could be assumed that the processes discussed in the present paper for HgIII, CuII and AgII excited states have the same nature, even though electron excitation is considered.

Acknowledgement. The authors thank the Bulgarian National Science Foundation for financial support under 475/1994 contract.

References

1. H.J. Gerritsen, P.V. Goedertier: J. Appl. Phys. **35**, 3060 (1964)
2. H.R. Lathi, W. Seelig, A. Stadler: IEEE J. QE-**5**, 317 (1976)
3. J.R. McNeil, J. Collins, K.B. Persson, D.L. Franzen: Appl. Phys. Lett. **27**, 595 (1975)
4. R. Solanki, E.L. Latuch, W.M. Fairbank, Jr., G.J. Collins: Appl. Phys. Lett. **34**, 568 (1979)
5. K. Jain, S.A. Newton: Appl. Phys. B **26**, 43 (1981)
6. E. Alipieva, K. Blagoev, N. Dimitrov: Opt. Spectr. (in Russian) **66**, 1212 (1988)
7. C.E. Moor: Atomic Energy Levels, Vol. III, p. 198, NSRDS-NBS 467 (May 1958)
8. E.W. Foster: Proc. Roy. Soc. A **200**, 429 (1950)
9. K. Blagoev, N. Dimitrov: Phys. Lett. A **117**, 185 (1986)
10. K. Blagoev, N. Dimitrov, A. Benhalla, P. Bogdanovich, A. Momkauskaite, Z.B. Rudzikas: Physica Scripta **41**, 213 (1990)
11. K. Blagoev, Yu. Stoyanova N. Dimotrov: Proc. 23rd EGAS TORUN, 87 (1991)
12. D.J. Beideck, L.J. Curtis, R.E. Irving, S.T. Maniak, R. Hellborg, S.G. Johansson, A.A. Joueizadeh, I. Martinson, T. Brage: Phys. Rev. A **47**, 884 (1993)
13. R.A. Phaneuf, P.O. Tayor, G.H. Dunn: Phys. Rev. **14**, 2021 (1976)
14. I.I.. Gudzenko, S.I. Yakovlenko: Plasma's laser (in Russian) (Atomizdat, Moscow 1978) pp. 6–251
15. E.E. Nikitin, B.M. Smirnov Atomic-molecule processes (in Russian) (Moscow, 1988)
16. I. McDanial, E. Mezon: Mobility and diffusion of ions into gases (in Russian) (Mir, Moscow 1976) pp. 5–420
17. R.G. Carman, A. Maitland: J. Phys. D: Appl. Phys. **20**, 1021 (1987)
18. R.R. Arslanbekev, A.A. Kudryavtzev, I.A. Movchan JTF (in Russian) **62**, 116 (1992)
19. J.R. McNeil, G.J. Collins, F.J. DeHoog: J. Appl. Phys. **50**, 6183 (1979)
20. D.R. Bates: Atomic and Molecular Processes (Academic Press, New York 1962)
21. Yu.M. Smirnov: Opt. Spectr (in Russian) **59**, 768 (1985)
22. E.K. Karabut, V.F. Kravchenko, V.F. Papakin: J. Appl. Sp. (in Russian) **XIX**, 145 (1973)
23. G.J. Fetzer, J.J. Rocca, G.J. Collins, R. Jacobs: J. Appl. Phys. **60**, 2739 (1986)
24. D.J. Walker, C.P.J. Barty, G.Y. Yin, J.F. Young, S.E. Harris: Opt. Lett. **12**, 894 (1987)
25. A.J. Mendelsohn, S.E. Harris: Opt. Lett. **10**, 128 (1985)